

# Synthesis of $\text{Sr}_x\text{Ba}_{(1-x)}\text{TiO}_3$ Solid Solutions from the Mechanically Activated System $\text{BaCO}_3$ - $\text{SrCO}_3$ - $\text{TiO}_2$

V. Berbenni and A. Marini

CSGI - Dipartimento di Chimica Fisica dell' Università di Pavia,  
Viale Taramelli 16, 27100 Pavia, Italy

Reprint requests to Dr. V. Berbenni. Fax: 0039-0382-507575. E-mail: [berbenni@matsci.unipv.it](mailto:berbenni@matsci.unipv.it)

Z. Naturforsch. **57 b**, 859–864 (2002); received March 21, 2002

Mechanical Activation, Barium Strontium Titanate, Solid State Reactions

Mixtures  $x\text{SrCO}_3$  (1 -  $x$ ) $\text{BaCO}_3$   $\text{TiO}_2$  ( $0 < x < 1$ ) have been mechanically activated by high energy milling in order to promote the formation of mixed (Sr,Ba) carbonate that decomposes, in a single stage, at temperatures generally lower than for the corresponding physical mixtures. By annealing such milled mixtures at high temperatures ( $\approx 1000$  °C), cubic solid solutions  $\text{Sr}_x\text{Ba}_{(1-x)}\text{TiO}_3$  are obtained (except at  $x = 0.1$  where a tetragonal solid solution forms) whose lattice parameters decrease linearly with  $x$ . The enthalpy of solid solution formation changes with composition showing higher values in the  $x$  range between  $x = 0.2$  and  $0.5$  where the reaction has been demonstrated to occur via the formation of  $\text{Ba}_2\text{TiO}_4$ . By contrast, the enthalpy values decrease for  $x > 0.5$ .

## Introduction

Alkaline earth metal titanates have become very important in the ceramic and electronic industries where, in particular,  $\text{BaTiO}_3$  and  $\text{SrTiO}_3$  are widely employed.  $\text{BaTiO}_3$  is finding application because of its high dielectric constant, ferroelectric properties and positive temperature coefficient of electrical resistivity [1].  $\text{SrTiO}_3$  is employed as a substrate for the heteroepitaxial growth of high- $T_c$  superconductors [2 - 4]. Moreover (Ba,Sr) $\text{TiO}_3$  solid solutions are used in chemical sensors [5], multi-layer capacitors and DRAM devices [6 - 8].

In the past both  $\text{BaTiO}_3$  and  $\text{SrTiO}_3$  have been synthesized by high temperature solid state reactions between Ba/Sr carbonates or hydroxides and  $\text{TiO}_2$ . However, this procedure can result in ceramics with compositional inhomogeneities and/or excessive grain growth. Indeed for the mentioned applications, these materials have to be prepared highly homogeneous both as regards composition and particle size. Hence the intimate mixing of the starting powders is of vital importance for their preparation. Several preparative methods have been proposed that allow such an intimate mixing to be realized through additional steps prior to the final annealing phase: oxide coprecipitation [9], sol-gel route [10], thermal decomposition of oxo-salts [11, 12], and hydrothermal methods [13 - 14]. Re-

cently Poth *et al.* [15] have devised a combustion-synthesis of  $\text{SrTiO}_3$ . Many of these methods, besides requiring additional processing before annealing, use solvents that have to be disposed properly.

Moreover, since several applications of titanates envisage the introduction of evenly distributed dopant(s) to enhance a particular property [16], the mechanical milling should not be overlooked as a synthetic route. Indeed room temperature mechanochemical synthesis of both  $\text{BaTiO}_3$  and  $\text{SrTiO}_3$  has been performed by milling the oxides under vacuum [17] with the disadvantage that alkaline earth oxides had to be calcined ( $\approx 90$  h at  $1300$  °C) to decompose the hydroxide / carbonate layers formed during storage. Recently Xue *et al.* [18] reported a breakthrough by successfully performing a room temperature synthesis by milling under nitrogen a mixture of Ba/Ti oxides.

Our research has recently dealt with the mechanical activation of solid state reactions in oxide systems. Work has been performed on the formation reaction of barium and strontium ferrites [19, 20], and another paper [21] reports the results obtained in setting up a preparative method of  $\text{BaTiO}_3$  by milling and annealing mixtures of  $\text{BaCO}_3$  and  $\text{TiO}_2$  (rutile). Furthermore the solid state reactions occurring in the mechanically activated system  $\text{SrCO}_3$  -  $\text{TiO}_2$  (rutile) have been studied [22].

This work is dealing with the preparation of  $\text{Sr}_x\text{Ba}_{(1-x)}\text{TiO}_3$  solid solutions ( $0 < x < 1$ ) starting from mechanically activated mixtures  $\text{SrCO}_3$ - $\text{BaCO}_3$ - $\text{TiO}_2$  (rutile). Experimental results are also reported on their thermochemical and structural characterisation.

## Experimental

### 1. Starting chemicals and samples preparation

The starting chemicals were purchased from Aldrich Chimica (Italy):  $\text{BaCO}_3$  (Purity + 99%),  $\text{SrCO}_3$  (Purity + 99%) and  $\text{TiO}_2$  (predominantly rutile as it has been demonstrated by taking the XRD patterns, purity 99.9%). Physical mixtures of composition  $\text{Sr}_x\text{Ba}_{(1-x)}\text{TiO}_3$  [ $x$  from 0 to 1.0 in steps of 0.1] were prepared by weighing the appropriate amounts of the components and by mixing them manually in an agate mortar for 10 min. Afterwards the powders were suspended in acetone under magnetic stirring for 3 h and the solvent allowed to evaporate in an oven at 60 °C.

The physical mixtures were dry milled for 80 h in a high energy planetary mill (Pulverisette 7 by Fritsch, Germany) at 400 rpm rotation speed with 4 agate balls (12 mm diameter) in an agate jar. The ball/sample mass ratio was 10:1. After the allotted time the jars were opened and the samples were scraped from the jars: henceforth we will refer to these samples as milled or mechanically activated mixtures. Finally they were subjected to the annealing procedures described in the following.

Fig. 1 shows the XRD patterns of the milled mixtures. The angular regions between  $2\theta \approx 23^\circ$  and  $26^\circ$  and  $33^\circ$  and  $37^\circ$  are worth to be briefly commented on. The peaks

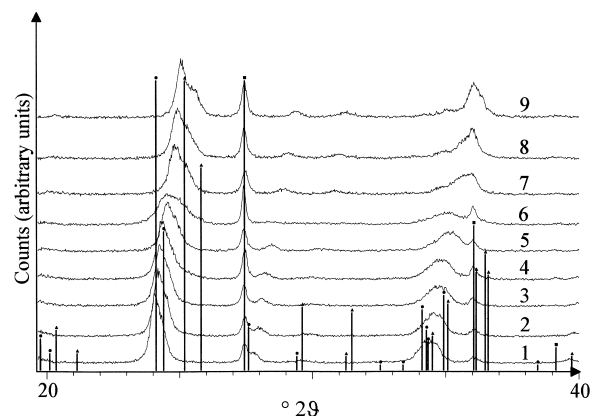


Fig. 1. XRD powder patterns of ball milled mixtures. ●  $\text{BaCO}_3$  JCPDS card n. 41-0373; ■  $\text{TiO}_2$  JCPDS card n. 21-1276; ▲  $\text{SrCO}_3$  JCPDS card n. 05-0418.  $-x$  starts from 0.1 (pattern 1) and increases up to 0.9 (pattern 9) in steps of 0.1.

in these regions are broad as a consequence of overlapping carbonate reflexions. The milling does not result in any reaction with  $\text{TiO}_2$ , as it can be deduced from the presence of the 100% rutile peak ( $2\theta \approx 27.4^\circ$ ) in the entire composition range, but it seems that solid solution between the carbonates occurred as it is the case with carbonate coprecipitation from solutions of Sr and Ba nitrates [23].

### Experimental Techniques

- TGA Measurements were performed with the 2950 thermogravimetric analyser (TA Instruments Inc. USA) connected to the TA5000 computer (also by TA Instruments Inc. USA). About 50 mg samples (both physical and milled mixtures) were placed in a Pt sample holder and heated at 2 K/min under a nitrogen flow of 100 ml/min from 25 up to 850 °C. An isothermal stage of 12 h was appended at the end of the ramp.

- Simultaneous DSC / TGA measurements were performed with a SDT apparatus (SDT by TA Instruments Inc. USA) connected to the TA5000 computer. About 35 mg samples of the milled mixtures were placed in a Pt pan and heated, under a nitrogen flow of 120 ml/min, at 5 K/min from room temperature to 1100 °C. The enthalpies of the relevant reactions were determined from the area of the peaks and referred to the reaction extent that has been calculated from the mass loss under the peak. DSC Calibration was performed using sapphire and gold as standards.

- X-ray diffraction patterns of the thermally treated samples (both in TGA and TGA-DSC) were taken by putting the samples on a non diffracting silicon slide. Use was made of an X-ray powder diffractometer (Bruker D5005) equipped with a goniometer and a graphite bent crystal monochromator. XRD patterns were recorded in step scan mode (step  $0.02^\circ$ , 3 s/step,  $2\theta$  range 20 - 70 °; 40 kV, 40 mA).

- About 200 mg samples of the milled mixtures were heated in a tubular furnace (Carbolite MTF 12/38/400) at 5 K/min up to 1100 °C and then were let to cool down to room temperature. X-ray diffraction patterns of these samples were taken by putting them on a non diffracting silicon slide. The patterns were recorded in step scan mode (step  $0.02^\circ$ , 8 s/step,  $2\theta$  range 10 - 120°; 40 kV, 40 mA). From the XRD patterns the lattice parameters of solid solutions have been calculated by a least squares refinement procedure. On these samples DSC measurements were performed (DSC 2920 by TA Instruments Inc. USA) at 10K/min between -100 and 160 °C.

## Results and Discussion

Fig. 2 shows as an example the TGA curves of the  $x \text{SrCO}_3 \cdot (1-x) \text{BaCO}_3 \cdot \text{TiO}_2$  mixture ( $x = 0.2$ )

$x$	$\Delta_{\text{calc}}M$ (%)	$\Delta_{\text{tot}}M^{\text{PM}}$ (%)	$\Delta_{\text{tot}}M^{\text{BM}}$ (%)	$\alpha_{\text{dyn}}^{\text{PM}}$	$\alpha_{\text{dyn}}^{\text{BM}}$
0.1003	-16.17	-16.15	-16.55	0.8504	1.0000
0.2004	-16.42	-16.33	-16.67	0.9088	1.0000
0.3000	-16.78	-16.66	-17.21	0.6669	1.0000
0.4037	-17.17	-17.00	-17.99	0.7324	1.0000
0.5000	-17.44	-17.30	-18.45	0.7682	0.8461
0.5999	-17.80	-17.62	-18.53	0.7928	0.8190
0.7003	-18.17	-18.03	-18.87	1.000	1.0000
0.7997	-18.53	-18.53	-19.35	0.8249	1.0000
0.8999	-18.94	-18.62	-19.75	1.0000	1.0000

Table 1. TGA data of milled and physical mixtures.  $\Delta_{\text{calc}}M$  (%) is the calculated mass loss (see text),  $\Delta_{\text{tot}}M^{\text{PM}}$  and  $\Delta_{\text{tot}}M^{\text{BM}}$  are the experimental mass losses (%) of physical (PM) and ball milled (BM) mixtures.  $\alpha_{\text{dyn}}$  is the ratio of the dynamic (*i. e.* up to 850 °C) to the total mass losses. The superscripts PM and BM indicate physical and milled mixtures, respectively.

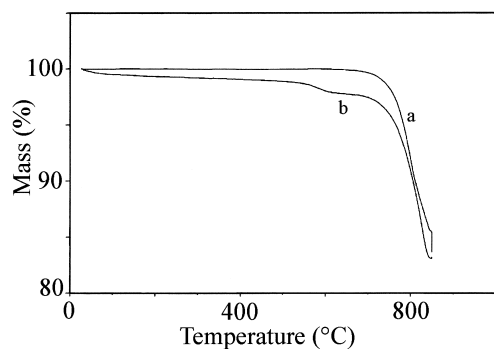


Fig. 2. TGA curve of the 0.2  $\text{SrCO}_3$  · 0.8  $\text{BaCO}_3$  ·  $\text{TiO}_2$  mixture: a) Physical mixture; b) mixture ball milled for 85 h.

both physically (2a) and ball milled (2b). From the early mass loss of the milled sample it can be argued that water absorption occurs during milling. This in turn explains the greater mass loss of the milled sample at the end of the run. Moreover the mass loss step around 600 °C is likely due to Sr hydrogenocarbonate decomposition which forms during milling [22]. Another effect of milling is the lowering of the mass loss temperature: while, in the physical mixtures, an appreciable amount of mass loss occurs during the 12 h isothermal period, for the milled mixtures the mass loss is finished within 850 °C. Such an effect does not occur to the same extent over all the composition range: indeed the TGA data of both physically and milled mixtures are summarized in Table 1 where the ratio ( $\alpha_{\text{dyn}}$ ) of the mass loss up to 850 °C with respect to the mass loss at the end of the run is shown. This parameter is always greater for the milled mixtures than for the physical ones for  $x$  up to 0.5. The difference is at a maximum at  $x = 0.3$  whereas it decreases for  $x > 0.5$ .

Hence the TGA measurements have shown that mechanical activation lowers the decomposition temperature more for the Ba- than for the Sr-rich

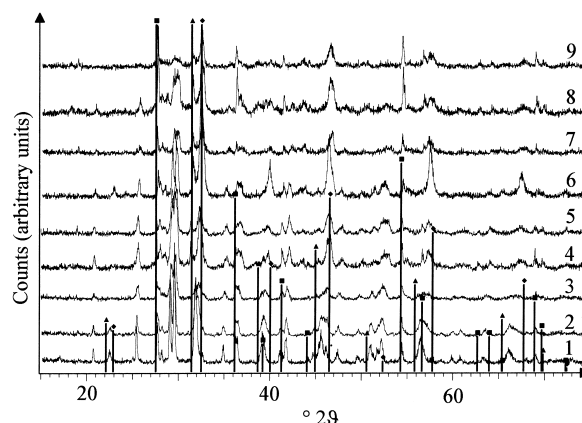


Fig. 3. XRD powder patterns of physical mixtures  $x\text{SrCO}_3$  ·  $(1-x)\text{BaCO}_3$  ·  $\text{TiO}_2$  ( $0 < x < 1$ ) annealed at 850 °C for 12 h.  $\blacktriangle$   $\text{BaTiO}_3$  JCPDS card n. 31-0174;  $\blacksquare$   $\text{TiO}_2$  JCPDS card n. 21-1276;  $\blacklozenge$   $\text{SrTiO}_3$  JCPDS card n. 35-0734;  $x$  starts from 0.1 (pattern 1) and increases up to 0.9 (pattern 9) in steps of 0.1.

compositions. However, the carbonate decomposition takes place in a single stage over the entire composition range.

A deeper insight into the effect of mechanical milling on  $\text{Sr}_x\text{Ba}_{(1-x)}\text{TiO}_3$  formation is obtained by comparison of the XRD powder patterns of the TGA annealed samples. Fig. 3 shows the XRD patterns of the annealed physical mixtures. The following remarks can be made:

- All samples show the presence of unreacted  $\text{TiO}_2$  (see the peaks at  $2\theta \approx 27.5^\circ$ ,  $36^\circ$  and  $54.2^\circ$ ).
- The samples with  $x$  between 0.4 and 0.9 show with 100% intensity the peak characteristic of  $\text{Sr}_2\text{TiO}_4$  ( $2\theta \approx 31.2^\circ$ ).
- All samples except for that with  $x = 0.9$  show reflexions (at  $2\theta \approx 25.3^\circ$  and  $29 - 29.5^\circ$ ) characteristic of  $\text{Ba}_2\text{TiO}_4$ .
- The samples with  $x$  up to 0.3 show at  $2\theta \approx 32 - 33^\circ$  a single peak (though rather broad for  $x = 0.2$

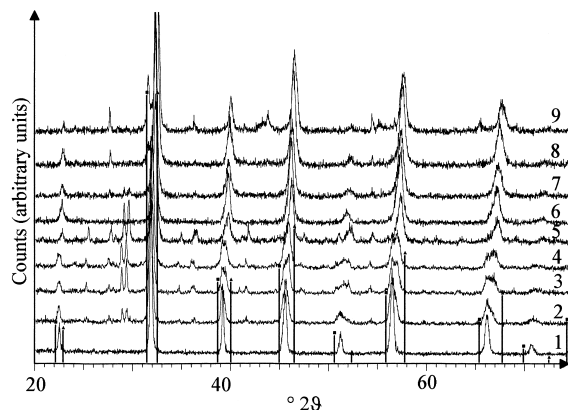


Fig. 4. XRD powder patterns of ball milled mixtures  $x\text{SrCO}_3 \cdot (1-x)\text{BaCO}_3 \cdot \text{TiO}_2$  ( $0 < x < 1$ ) annealed at  $850^\circ\text{C}$  for 12 h. ■  $\text{BaTiO}_3$  JCPDS card n. 31-0174; ▲  $\text{SrTiO}_3$  JCPDS card n. 35-0734 –  $x$  starts from 0.1 (pattern 1) and increases up to 0.9 (pattern 9) in steps of 0.1.

and 0.3) lying between the 100% intensity markers of  $\text{SrTiO}_3$  and  $\text{BaTiO}_3$ .

e) The samples with  $x > 0.3$  show peaks, quite broad in some instances, at  $2\theta \approx 40^\circ, 46.5^\circ, 57.8^\circ, 67.8^\circ$  characteristic of  $\text{SrTiO}_3$ .

In summary, the solid state reaction occurred in the physical mixtures appears to be largely incomplete since unreacted  $\text{TiO}_2$  remains along with significant amounts of  $\text{Ba}_2\text{TiO}_4$  and/or  $\text{Sr}_2\text{TiO}_4$  (depending on the initial composition).

Fig. 4 shows the XRD patterns of the annealed milled mixtures. The following remarks apply:

a) The  $x = 0.1$  mixture shows only peaks lying between the markers of  $\text{BaTiO}_3$  and  $\text{SrTiO}_3$ . No unreacted  $\text{TiO}_2$  is present.

b) Some unreacted  $\text{TiO}_2$  is present in the  $x = 0.2$  mixture besides some weak peaks characteristic of  $\text{Ba}_2\text{TiO}_4$ . The other peaks are (as for the mixture with  $x = 0.1$ ) lying between the markers of  $\text{BaTiO}_3$  and  $\text{SrTiO}_3$ .

c) The samples with  $x = 0.3, 0.4$  and  $0.5$  show that rather incomplete reactions have taken place. Indeed these samples exhibit peaks of  $\text{TiO}_2$  and  $\text{Ba}_2\text{TiO}_4$  the intensities of which increase with  $x$ . Furthermore the peaks between the markers of  $\text{BaTiO}_3$  and  $\text{SrTiO}_3$  are quite broad.

d) The samples with  $x = 0.6$  and  $0.7$  only show peaks between the markers of  $\text{SrTiO}_3$  and  $\text{BaTiO}_3$ .

e) The two Sr-richest mixtures show, in addition to peaks next to  $\text{SrTiO}_3$  markers, minor amounts

Table 2. Simultaneous TGA/DSC data of milled and physical mixtures.  $\Delta_r H$  are the reaction enthalpies (kJ/mole of solid solution formed) for physical (PM) and ball milled (BM) mixtures, respectively.  $\Delta_{\text{peak}} M$  (%) are the mass losses under the corresponding DSC peaks.

$x$	$\Delta_r H^{\text{PM}}$	$\Delta_{\text{peak}} M^{\text{PM}}$	$\Delta_r H^{\text{BM}}$	$\Delta_{\text{peak}} M^{\text{BM}}$
0.1003	307.4	-15.87	577.6	-15.78
0.2004	320.5	-16.26	703.4	-15.80
0.3000	318.2	-16.47	735.6	-16.28
0.4037	328.3	-17.02	729.2	-16.80
0.5000	386.2	-17.35	721.6	-16.85
0.5999	354.4	-17.46	649.3	-17.28
0.7003	351.3	-17.80	632.9	-17.46
0.7997	264.4	-18.10	603.7	-18.20
0.8999	289.8	-18.56	572.6	-18.37

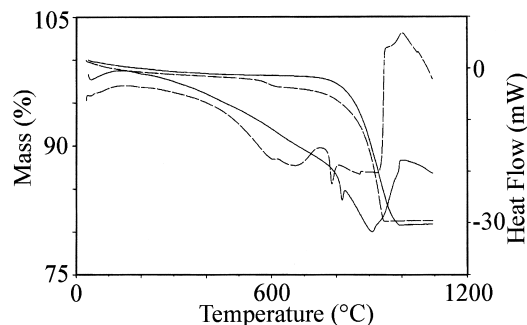


Fig. 5. Simultaneous DSC/TGA curve of the  $0.5\text{SrCO}_3 \cdot 0.5\text{BaCO}_3 \cdot \text{TiO}_2$  mixture. Full lines: signals of the physical mixture. Dashed lines: signal of the mixture ball milled 85 h.

of unreacted rutile and, as a consequence, they exhibit the 100% intensity reflexion of  $\text{Sr}_2\text{TiO}_4$  ( $2\theta \approx 31.2^\circ$ ).

In the case of the milled mixtures the annealing causes the reaction to proceed further than in the case of the annealed physical mixtures. In some instances ( $x = 0.1, 0.2, 0.6$  and  $0.7$ ) the only peaks present are those between the markers of  $\text{SrTiO}_3$  and  $\text{BaTiO}_3$  so allowing one to conclude that a mixed (Sr,Ba) titanate is the final product. However, for other mixture compositions,  $\text{Ba}_2\text{TiO}_4$  ( $x = 0.3, 0.4$  and  $0.5$ ) and  $\text{Sr}_2\text{TiO}_4$  ( $x = 0.8$  and  $0.9$ ) are also present that could have been formed as intermediates leading to the formation of mixed Ba / Sr titanates.

The effect of mechanical activation has been examined also by simultaneous TGA-DSC. Fig. 5 shows, as an example, the DSC/TGA curves of the  $x\text{SrCO}_3 \cdot (1-x)\text{BaCO}_3 \cdot \text{TiO}_2$  ( $x = 0.5$ ) system both physical (full line) and milled (dashed line).

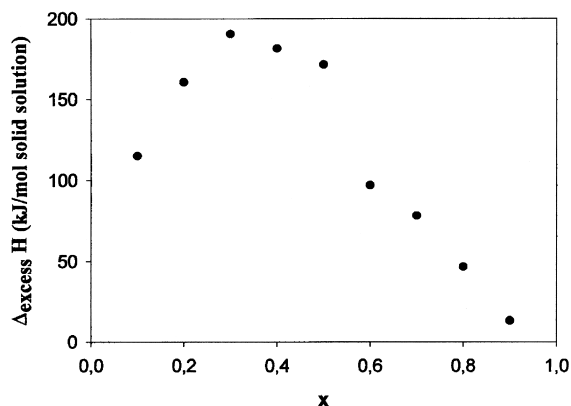


Fig. 6. Differences between experimental and calculated reaction enthalpies (see text) as a function of mixture composition ( $x$ ).

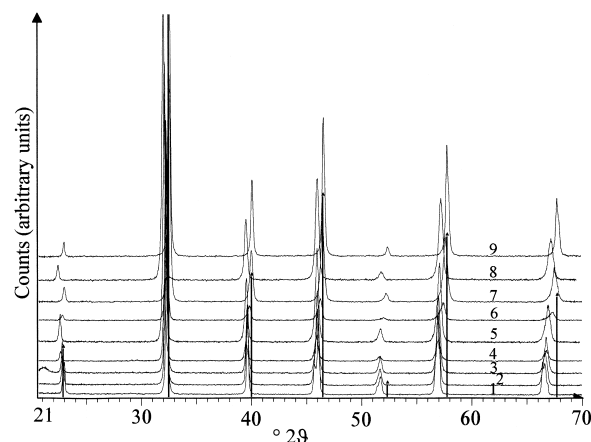


Fig. 7. XRPD of  $\text{Sr}_x\text{Ba}_{(1-x)}\text{TiO}_3$  samples prepared by heating the milled mixtures at 5 K/min up to 1100 °C. –  $x$  starts from 0.1 (pattern 1) and increases up to 0.9 (pattern 9) in steps of 0.1.

The DSC curve of the milled mixture deviates from the baseline at about 400 °C showing that an endothermic process is going on that is not taking place yet in the physical mixture. Table 2 gives the reaction enthalpy data along with the mass loss values (for both physical and milled mixtures). Simultaneous TGA/DSC runs have been performed under the same experimental conditions on the milled mixtures  $\text{SrCO}_3\text{-TiO}_2$  and  $\text{BaCO}_3\text{-TiO}_2$ : reaction enthalpies of 561.9 kJ/mol  $\text{SrCO}_3$  and 537.8 kJ/mol  $\text{BaCO}_3$  were obtained for the formation of  $\text{SrTiO}_3$  and  $\text{BaTiO}_3$ , respectively. By taking into account the relative amounts of Sr and Ba carbonates contained in the different mixtures, enthalpy values can be calculated that are, at all compositions, lower

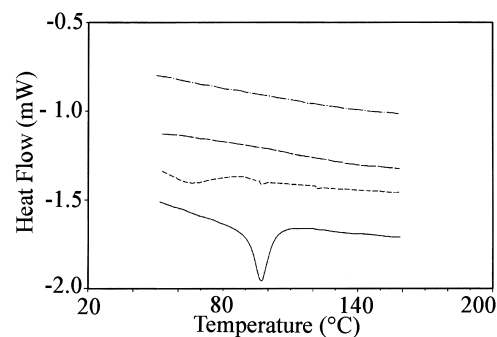


Fig. 8. — DSC curves of  $\text{Sr}_x\text{Ba}_{(1-x)}\text{TiO}_3$  samples prepared by heating the milled mixtures at 5 K/min up to 1100 °C. Full line  $x = 0.1$ ; short dashed line  $x = 0.2$ ; long dashed line  $x = 0.3$ ; dash-dotted line  $x = 0.4$ .

that the experimental ones ( $\Delta_r H^{\text{BM}}$  in Table 2). The differences ( $\Delta_{\text{excess}} H$ ) are given in Fig. 6 and are likely due to the formation of solid solutions. They are larger for  $x$  between 0.2 and 0.5. It has been noted previously that, at these compositions, significant amounts of  $\text{Ba}_2\text{TiO}_4$  are formed by annealing at 850 °C (see Fig. 4). The formation of barium orthotitanate as an intermediate of the mixed  $(\text{Ba,Sr})\text{TiO}_3$  is mirrored by the excess reaction energy intake at these compositions. As a matter of fact, the difference is quite low for  $x = 0.1$ , *i. e.* when no  $\text{Ba}_2\text{TiO}_4$  is formed by annealing at 850 °C, and it sharply decreases for increasing  $x$  beyond 0.5 where again no  $\text{Ba}_2\text{TiO}_4$  formed by annealing at 850 °C.

The samples of  $\text{Sr}_x\text{Ba}_{(1-x)}\text{TiO}_3$  solid solutions were characterized from a structural point of view. It is known that a phase transition occurs in pure  $\text{BaTiO}_3$  from a tetragonal (ferroelectric) to a cubic (paraelectric) phase at about 120 °C [24]. The transition temperature decreases almost linearly from 120 °C ( $\text{BaTiO}_3$ ) to –231 °C ( $\text{SrTiO}_3$ ). Wechsler and Kirby [25] demonstrated this transition by performing DSC experiments on samples of solid solutions (with  $x$  up to 0.07) prepared at 1400 °C by solid state reaction, and the presence of a tetragonal phase could also be confirmed [26] by a small tetragonal distortion of the perovskite structure of the solid solution. The samples prepared by heating the milled mixtures at 5 K/min up to 1100 °C gave the XRD patterns shown in Fig. 7: the peaks are at angular positions characteristic of the cubic phase ( $\text{SrTiO}_3$  perovskite) and also the relative intensities of the peaks agree fairly well with those of the perovskite. Only the peaks of the  $x = 0.1$  mixture

Table 3. Lattice parameter values of  $\text{Sr}_x\text{Ba}_{1-x}\text{TiO}_3$  solid solutions obtained by least squares refinement of the value of the cubic lattice parameter of  $\text{SrTiO}_3$  ( $a = 3.905 \text{ \AA}$  characteristic of cubic  $\text{SrTiO}_3$  – see the JCPDS card n. 35-0734).

$x$	$a$ (Å)	$x$	$a$ (Å)
0.2004	3.980(5)	0.3000	3.969(5)
0.4037	3.961(5)	0.5000	3.946(5)
0.5999	3.924(5)	0.7003	3.932(4)
0.7997	3.924(4)	0.8999	3.913(4)

show a tetragonal distortion and, correspondingly, a DSC measurement performed on this very sample showed the tetragonal  $\rightarrow$  cubic transition peak (see Fig. 8 where the DSC scans performed on the mixtures with  $x$  up to 0.4 are shown for sake of comparison). The cubic cell parameters of the solid solutions have been determined by a least squares refinement procedure and are reported in Table 3. The values decrease linearly with  $x$  according to the equation (Vegard's law):  $a$  (Å) =  $3.9957 - 0.09534x$  ( $r = -0.96416$ ).

## Conclusions

Mixtures  $x \text{ SrCO}_3 (1 - x) \text{ BaCO}_3 \text{ TiO}_2$  ( $0 < x < 1$ ) have been mechanically activated by milling and then annealed up to different temperatures. The effect of ball milling is to promote the formation of mixed (Sr, Ba) carbonate that decomposes in a single stage and at temperatures generally lower than those of the corresponding physical mixtures. Such a temperature effect is most apparent in the Ba-rich mixtures ( $x$  up to 0.4). Cubic solid solutions  $\text{Sr}_x\text{Ba}_{(1-x)}\text{TiO}_3$  have been obtained at all compositions but at  $x = 0.1$  (where a tetragonal solid solution is obtained). The cubic lattice parameter decreases linearly with  $x$  (according to Vegard's law) as the smaller  $\text{Sr}^{2+}$  ion (ionic radius 113 pm) enters the structure substituting for the larger  $\text{Ba}^{2+}$  ion (ionic radius 135 pm). The enthalpy of the solid solution formation changes with composition and shows higher values in the  $x$  range between  $x = 0.2$  and 0.5 where the reaction has been demonstrated to occur via the formation of  $\text{Ba}_2\text{TiO}_4$  as an intermediate. The enthalpy values sharply decrease on increasing the  $x$  value beyond 0.5.

- [1] P. P. Phule, S. H. Risbud, J. Mater. Sci. **25**, 1169 (1990).  
 [2] D. G. Shlom, A. F. Marshall, Z. J. Sizemore, J. N. Chen, I. Bozovic, K. E. von Dessenneck, J. S. Harris, J. C. Bravman (Jr.), J. Cryst. Growth **102**, 361 (1990).  
 [3] T. Terashima, Y. Bando, K. Iijima, K. Yamamoto, K. Hirata, K. Kamigaki, H. Terauchi, Phys. Rev. Lett. **65**, 2684 (1990).  
 [4] M. Kawai, S. Watanabe, T. Hanada, J. Cryst. Growth **112**, 745 (1991).  
 [5] Y. C. Yeh, T. Y. Tseng, J. Mat. Sci. Lett. **7**, 766 (1998).  
 [6] D. Chambonnot, C. Andry, A. Fages-Bonnery, C. Mer, C. Fages, J. Perriere, J. Phys. Fr. **8**, 213 (1998).  
 [7] A. I. Dedyk, S. F. Karmanenko, S. Leppavuori, V. I. Sakharov, J. Phys. Fr. **8**, 217 (1998).  
 [8] S. Hoffmann, R. Waser, J. Phys. Fr. **8**, 221 (1998).  
 [9] M. I. Yanovskaya, N. V. Golubko, E. A. Nenasheva, Inorg. Mat. **32**, 200 (1996).  
 [10] J. Liao, M. Senna, Mater. Res. Bull. **30**, 385 (1995).  
 [11] G. Pfaff, Ceram. Int. **20**, 111 (1994).  
 [12] M. A. Sekar, G. Dhanaraj, H. L. Phat, K. C. Patil, J. Mat. Sci., Mat. Electr. **3**, 237 (1992).  
 [13] M. Leoni, M. Viviani, P. Nanni, V. Buscaglia, J. Mat. Sci. Lett. **15**, 1302 (1996).  
 [14] A. T. Chien, J. S. Speck, F. F. Lange, A. C. Daykin, C. G. Levi, J. Mat. Res. **10**, 1784 (1995).  
 [15] J. Poth, R. Haberkorn, H. P. Beck, J. Europ. Ceram. Soc. **20**, 707 (2000).  
 [16] G. F. Everson in "Speciality Inorganic Chemicals", ed. by R. Thompson, Special Publication 40, p. 226, Royal Society of Chemistry, London (1981).  
 [17] N. J. Welham, J. Mater. Res. **13**, 1607 (1998).  
 [18] J. Xue, J. Wang, D. Wan, J. Am. Ceram. Soc. **83**, 232 (2000).  
 [19] V. Berbenni, A. Marini, N.J. Welham, P. Galinetto, M.C. Mozzati, J. Eur. Cer. Soc., in press.  
 [20] V. Berbenni, A. Marini, Mater. Res. Bull. **37**, 221 (2002).  
 [21] V. Berbenni, A. Marini, G. Bruni, Thermochemica Acta **374**, 151 (2001).  
 [22] V. Berbenni, A. Marini, G. Bruni, J. Alloys Comp. **329**, 230 (2001).  
 [23] J. M. Criado, M. J. Dianez, M. Macias, M. C. Paradas, Thermochemica Acta **171**, 229 (1990).  
 [24] Werner Kanzig (ed.) in: Ferroelectrics and Antiferroelectrics, p. 179, Academic Press, New York 1957.  
 [25] B. A. Wechsler, K. W. Kirby, J. Am. Ceram. Soc. **75**, 981 (1992).  
 [26] W. Eiser, R. Haberkorn, H. P. Beck, J. Eur. Cer. Soc. **21**, 2319 (2001).